

Article

Engineering *Escherichia coli* for Poly- β -hydroxybutyrate Production from Methanol

Jiaying Wang^{1,2,3,†}, Zhiqiang Chen^{2,†} , Xiaogui Deng^{1,2,4}, Qianqian Yuan^{2,5,*} and Hongwu Ma^{2,5,*} ¹ Tianjin University of Science and Technology, Tianjin 300457, China² Biodesign Center, Key Laboratory of Engineering Biology for Low-Carbon Manufacturing, Tianjin Institute of Industrial Biotechnology, Chinese Academy of Sciences, Tianjin 300308, China³ College of Food Science and Engineering, Tianjin University of Science and Technology, Tianjin 300457, China⁴ School of Biological Engineering, Tianjin University of Science and Technology, Tianjin 300457, China⁵ National Center of Technology Innovation for Synthetic Biology, Tianjin 300308, China

* Correspondence: yuan_qq@tib.cas.cn (Q.Y.); ma_hw@tib.cas.cn (H.M.)

† These authors contributed equally to this work.

Abstract: The naturally occurring one-carbon assimilation pathways for the production of acetyl-CoA and its derivatives often have low product yields because of carbon loss as CO₂. We constructed a methanol assimilation pathway to produce poly-3-hydroxybutyrate (P3HB) using the MCC pathway, which included the ribulose monophosphate (RuMP) pathway for methanol assimilation and non-oxidative glycolysis (NOG) for acetyl-CoA (precursor for PHB synthesis) production. The theoretical product carbon yield of the new pathway is 100%, hence no carbon loss. We constructed this pathway in *E. coli* JM109 by introducing methanol dehydrogenase (Mdh), a fused Hps-phi (hexulose-6-phosphate synthase and 3-phospho-6-hexuloisomerase), phosphoketolase, and the genes for PHB synthesis. We also knocked out the *frmA* gene (encoding formaldehyde dehydrogenase) to prevent the dehydrogenation of formaldehyde to formate. Mdh is the primary rate-limiting enzyme in methanol uptake; thus, we compared the activities of three Mdhs in vitro and in vivo and then selected the one from *Bacillus methanolicus* MGA3 for further study. Experimental results indicate that, in agreement with the computational analysis results, the introduction of the NOG pathway is essential for improving PHB production (65% increase in PHB concentration, up to 6.19% of dry cell weight). We demonstrated that PHB can be produced from methanol via metabolic engineering, which provides the foundation for the future large-scale use of one-carbon compounds for biopolymer production.

Keywords: methanol condensation cycle; non-oxidative glycolysis; polyhydroxybutyrate; methanol; *Escherichia coli*; methanol dehydrogenase gene



Citation: Wang, J.; Chen, Z.; Deng, X.; Yuan, Q.; Ma, H. Engineering *Escherichia coli* for Poly- β -hydroxybutyrate Production from Methanol. *Bioengineering* **2023**, *10*, 415. <https://doi.org/10.3390/bioengineering10040415>

Academic Editors: Joana Rodrigues and Debora Ferreira

Received: 31 December 2022

Revised: 13 March 2023

Accepted: 20 March 2023

Published: 26 March 2023



Copyright: © 2023 by the authors. Licensee MDPI, Basel, Switzerland. This article is an open access article distributed under the terms and conditions of the Creative Commons Attribution (CC BY) license (<https://creativecommons.org/licenses/by/4.0/>).

1. Introduction

The increasing demand for energy and resources from rapid economic development has prompted research on possible alternatives. Some alternative sources, such as biogas, bioethanol, and biomethanol, have been widely produced from some waste materials [1,2]. Over 53 million tons of methanol, a potential, low-cost alternative substrate to sugar for bioindustries, is produced annually [3]. Studies on the use of methanol as a carbon source for the production of single-cell proteins, amino acids, and biopolymers have been intensively reported [4–7]. However, the commercial production of industrial chemicals from methanol using natural methylotrophs is limited mainly by the lack of well-developed genetic tools to implement synthetic pathways for objective products. Therefore, well-studied model strains, such as *Escherichia coli*, have gained great attention in the bioconversion of methanol [8]. There are three major natural pathways for methanol assimilation: the ribulose monophosphate (RuMP) cycle, the xylulose monophosphate (XuMP) cycle, and the serine cycle [9]. Among them, the RuMP cycle is considered the most applicable

methylotrophic pathway in *E. coli*, as the expression of only three heterologous enzymes is sufficient for methanol assimilation [10]. Muller et al. introduced three RuMP cycle enzymes, including methanol dehydrogenase (Mdh), hexulose-6-phosphate synthase (Hps), and 6-phospho-3-hexuloisomerase (Phi), into *E. coli* to enable methanol assimilation [10]. Whitaker et al. engineered the RuMP pathway and the flavanone naringenin synthesis pathway in *E. coli*, demonstrating the possibility of in vivo conversion of methanol into a specialty chemical [8].

Although the RuMP cycle is the most applicable methanol assimilation pathway in *E. coli*, methanol utilization via the RuMP pathway involves CO₂ loss and ATP expenditure in the synthesis of acetyl-CoA-derived products [11]. Specifically, three formaldehydes condense to pyruvate, which is decarboxylated to form acetyl-CoA and CO₂, thereby reducing the maximum carbon yield of acetyl-CoA to 67%. Similarly, two other methanol assimilation pathways—the serine pathway and the XuMP pathway—also reduce the carbon yield to 54% and 67%, respectively, which are not optimal pathways for maximizing the yields of acetyl-CoA-derived metabolites [12]. To solve this carbon-loss problem, Bogorad et al. [11] designed a new methanol assimilation pathway, referred to as the methanol condensation cycle (MCC), which consists of RuMP with a non-oxidative glycolysis (NOG) pathway and can produce one molecule of acetyl-CoA from two molecules of methanol without carbon loss. This new pathway allows the efficient conversion of methanol to multi-carbon acetyl-CoA-derived chemicals with 100% theoretical carbon yield.

As a derivative product of acetyl-CoA, poly-3-hydroxybutyrate (PHB) has excellent biodegradability. Within a certain period of time, microorganisms can break down PHB into CO₂ and H₂O, resulting in a significant reduction in “white pollution” [13,14]. PHB also has very good biocompatibility and is mainly used in drug delivery carriers and biological tissue engineering [15–17]. Additionally, recent studies have indicated that not only is PHB crucial for carbon storage, but it also plays an important role in supporting bacterial survival under adverse conditions, such as intermediate metabolite toxicity [18]. To this end, in this study, we aim to engineer the MCC pathway in *E. coli* and convert methanol to the acetyl-CoA-derived product PHB. An extended metabolic network model of *E. coli* incorporating the methanol assimilation pathway and the PHB synthesis pathway is used to identify the optimal pathway. Then, the functional modules for methanol assimilation, PHB synthesis, and NOG are introduced into *E. coli*, thereby constructing the entire bioconversion pathway from methanol to PHB.

2. Materials and Methods

2.1. Metabolic Network Analysis

An extended genome-scale *E. coli* metabolic network model based on iML1515 was used to calculate the optimal production pathway and yield of PHB by performing flux balance analysis (FBA) [19,20]. PHB is a polymer; thus, the monomer 3-hydroxybutyrate of PHB was considered the objective product in FBA. As no methanol utilization and MCC pathways exist in *E. coli*, the methanol utilization reaction converting methanol to formaldehyde and reactions of the MCC pathway (*Mdh*, *Hps-phi*, and *Fxp* (phosphoketolase)) were added to the iML1515 model. The FBA calculation was performed using the COBRApy [21]. In the calculation, the uptake rate of methanol was set to 6 mmol/gDCW/h. The non-growth-associated energy maintenance parameter was set to 0 mmol/gDCW/h.

2.2. Plasmid Construction

The primers used in the plasmid construction were obtained from GENEWIZ (Suzhou, China) and are listed in Table S1 (Supplementary Materials). The genes *mdh2* (GenBank: CP007739.1, protein ID: AIE59127.1) from *Bacillus methanolicus* MGA3, *mdh-CT* (GenBank: CP002878.1, protein ID: AEI80320.1) from *Cupriavidus necator* N-1 [22], and *TaADH* (GenBank: AL445067.1, protein ID: CAC12437.1) from *Thermoplasma acidophilum* DSM 1728 [23] were synthesized by Qinglan Biotech (Wuxi, China) with codon optimization and then cloned with primers 01, 02, 03, 04, 05, and 06 with restriction sites (Table 1, Column 3) at

the end. Then cloned genes were introduced into the pET-28a vector by enzyme-cut and linked up with corresponding restriction enzymes and ligases (TaKaRa, Kusatsu, Japan). The recombinant plasmids (Table 1) were confirmed by restriction mapping and sequencing (GENEWIZ, Suzhou, China). The confirmed constructs were subsequently transformed into *E. coli* BL21 (DE3) for protein expression. The fused Hps-phi gene was synthesized (Qinglan Biotech, Wuxi, China) according to the sequence reported by Orita et al. [24]. PCR experiments were performed using GoTaq DNA polymerase (TaKaRa, Kusatsu, Japan) with corresponding primers. Positive transformants were verified by colony PCR and Sanger sequencing.

2.3. Reconstruction of Expression Vector

Two T7 promoters in the expression vector pACYCDuet-1 were replaced by the *Trc* promoter from pTrc99a to reconstruct a new vector called pZQ for the C1 assimilation module according to Golden Gate cloning [25]. The vector pACYCDuet-1 was first lined by amplification from the position of the T7 promoter of the *mcs1* region with primers 09 and 10 (Table S1), which were designed to exclude the sequence of the T7 promoter. The lined sequence re-amplified by primers 11 and 12 (Table S1) was designed to contain the half sequence of the *Trc* promoter and the restriction site of the type IIs endonuclease *BsaI* (Thermo Fisher Scientific, Waltham, MA, USA). The re-amplified sequence was then re-circled by enzyme-cut and link-up with *BsaI* and T4 DNA-ligase (Thermo Fisher Scientific, Waltham, MA, USA). Finally, the re-circled plasmid was finally transformed to *E. coli* JM109, and positive vectors were verified by colony PCR and Sanger sequencing.

Similarly, the second T7 promoter was operated based on the first T7 promoter. The differences between the two were that (i) the initial vector was pACYCDuet-1, in which the T7 promoter changed to the *Trc* promoter, and (ii) the primers for the lining vector and re-amplifying primers (13, 14, 15, and 16; Table S1) were designed to be longer to avoid amplifying the *mcs1* region.

2.4. Gene Modules Construction

A C1 assimilation module was built by introducing methanol dehydrogenase (Mdh), hexulose-6-phosphate synthase (Hps), and 3-phospho-6-hexuloisomerase (Phi) into a reconstructed plasmid pZQ. Each methanol dehydrogenase gene (*mdh2*, *mdh-CT*, and *TaADH*) was first introduced into the multiple cloning site 1 of plasmid pZQ, individually with primers 17 and 18, 19 and 20, and 21 and 22, respectively (the restriction enzyme cutting sites are listed in Tables 1 and 2). The positive vectors were verified by colony PCR and Sanger sequencing. The multiple cloning site 2 of the vector pZQ with methanol dehydrogenase (Table 1) was added by Phs-Phi fusion with primers 23 and 24 (Table S1), and the positive vector was verified by colony PCR and Sanger sequencing, after which the C1 assimilation module was constructed.

The NOG module was constructed on plasmid PBHR68 containing the PHB production module [26]. The *fxpk* gene from *Bifidobacterium adolescentis* was introduced into PBHR68 by using primers 25 and 26 (Table 1) with enzyme cutting and combination.

Table 1. Plasmids used in this study. The first and second columns contain the plasmids and genes used in this study, respectively. The third column contains the plasmid information.

Plasmid	Encoded Gene	Description	Reference
pET-28a		High-copy-number, T7 promoter, pBR322 ori, Kan ^R	[27]
pET-28a_mdh2	<i>mdh2</i> gene from <i>B. methanolicus</i> MGA3	The <i>mdh2</i> gene was amplified from synthesized <i>mdh2</i> with codon optimization using primers 01 and 02 and ligated into the <i>NheI/BamHI</i> site of pET-28a.	[27]
pET-28a_mdh-CT	<i>mdh-CT</i> gene from <i>Cupriavidus necator</i> N-1	The <i>mdh-CT</i> gene was amplified from synthesized <i>mdh-CT</i> with codon optimization using primers 03 and 04 and ligated into the <i>NheI/HindIII</i> site of pET-28a.	This study

Table 1. Cont.

Plasmid	Encoded Gene	Description	Reference
pET-28a-TaADH	<i>TaADH</i> gene from <i>Thermoplasma acidophilum</i> DSM 1728	The <i>TaADH</i> gene was amplified from <i>Thermoplasma acidophilum</i> DSM 1728 using primers 05 and 06 and ligated into the <i>NheI/HindIII</i> site of pET-28a.	This study
pET-28a_hps-phi	The artificial fusion of <i>hps</i> and <i>phi</i> with codon optimization	The artificial fusion of the <i>hps</i> and <i>phi</i> genes was amplified using primers 07 and 08 and ligated into the <i>NdeI/XhoI</i> site of pET-28a.	This study
pACYCDuet-1 pTrc99a		High-copy-number, <i>T7</i> promoter, P15A ori, Cm ^R High-copy-number, <i>Trc</i> promoter, pBR322 ori, Amp ^R	Novagen Novagen
pZQ		The two <i>T7</i> promoters of pACYCDuet-1 were replaced by the <i>Trc</i> promoter of pTrc99a using primers 09, 10, 11, 12, 13, 14, 15, and 16 according to the method of GGA.	This study
pZQ_mdh2	<i>mdh2</i> gene from <i>B. methanolicus</i> MGA3	The <i>mdh2</i> gene was amplified from synthesized <i>mdh2</i> with codon optimization using primers 17 and 18 and ligated into the <i>BamHI/EcoRI</i> site of pZQ.	This study
pZQ_mdh2-hps-phi	<i>mdh2</i> gene from <i>B. methanolicus</i> MGA3 and artificial fusion of <i>hps</i> and <i>phi</i> with codon optimization	The artificial fusion of the <i>hps</i> and <i>phi</i> genes was amplified using primers 19 and 20 and ligated into the <i>NdeI/XhoI</i> site of pZQ_mdh2.	This study
pBHR68	<i>phaA</i> , <i>phaB</i> , and <i>phaC</i> from <i>Ralstonia eutropha</i>	<i>phaA</i> , <i>phaB</i> , and <i>phaC</i> expression plasmid, pBluescript SK ⁻ derivative, Amp ^R	[26]
pBHR70	<i>phaA</i> , <i>phaB</i> , <i>phaC</i> , <i>fbp</i> and <i>fxpk</i> from <i>Bifidobacterium adolescentis</i>	<i>phaA</i> , <i>phaB</i> , <i>phaC</i> , <i>fbp</i> and <i>fxpk</i> expression plasmid, pBluescript SK ⁻ derivative, Amp ^R	This study
pTKRED		pSC101 replication, <i>ParaBAD</i> -driven <i>I-SceI</i> gene, λ-Red, Sp ^R	[28]
pTKS/CS		p15A replication, LP regions, <i>I-SceI</i> restriction sites, Cm ^R , Tet ^R	[28]

2.5. Genome Manipulation

The wild-type JM109 and the previously constructed *E. coli* strain JM109-NOG were used as the chassis strain for further genome modification [29]. Plasmids pTKS/CS and pTKRED were used to delete the gene *frmA* (glutathione (GSH)-dependent formaldehyde dehydrogenase); this deletion method was conducted according to a 1-step inactivation of chromosomal genes [30]. The functions and description of plasmids (pTKS/CS and pTKRED) used for genome manipulation are listed in Table 1. Corresponding primers (27, 28, 29, 30, 31, and 32) are listed in Table S1. The strains used in this study are shown in Table 2.

Table 2. Strains used in this study. The first column reports the strains constructed in this study, the second column demonstrates the characteristics of the strains, and the third column shows the sources of these strains.

Strain	Feature	Source
JM109	<i>E. coli</i> , <i>recA1</i> , <i>endA1</i> , <i>gyrA96</i> , <i>thi</i> , <i>hsdR17</i> , <i>supE44</i> , <i>relA1</i> , Δ(<i>lac proAB</i>)/F' [<i>traD36</i> , <i>proAB</i> ⁺ , <i>lac</i> ^q <i>lacZΔM15</i>]	TransGen Biotech
BL21(DE3)	<i>E. coli</i> , F ⁻ , <i>ompT</i> , <i>gal</i> , <i>dcm</i> , <i>lon</i> , <i>hsdSB</i> (rB- mB-), λ(DE3 [<i>lacI lacUV5-T7 gene 1 ind1 sam7 nin5</i>])	TransGen Biotech
BL21-pet28a_mdh2	BL21(DE3), pet28a_mdh2	This study
BL21-pet28a_mdh-CT	BL21(DE3), pet28a_mdh-CT	This study
BL21-pet28a_TaADH	BL21(DE3), pet28a_TaADH	This study
BL21-pet28a_hps-phi	BL21(DE3), pet28a_hps-phi	This study
JM109-Δfrm	<i>E. coli</i> JM109, Δ <i>frmA</i>	This study
JM109-Δfrm-mdh2	JM109-Δfrm, pZQ_mdh2	This study
JM109-Δfrm-C1	JM109-Δfrm, pZQ_mdh2-hps-phi	This study
JM109-NOG	JM109, P _{<i>fbp</i>} ::P _{J23100} , :: <i>fxpk</i>	[29]

Table 2. Cont.

Strain	Feature	Source
JM109-NOG- Δ frm	JM109-NOG, Δ frmA	This study
JM109-NOG- Δ frm-PHB	JM109-NOG- Δ frm, pBHR68	This study
JM109-NOG- Δ frm-C1-PHB	JM109-NOG- Δ frm, pZQ_mdh2-hps-phi and pBHR68	This study
JM109- Δ frm-C1-PHB	JM109- Δ frm, pZQ_mdh2-hps-phi and pBHR68	This study
JM109-NOG- Δ frm-C1-PHB-NOG	JM109-NOG-frm, pZQ_mdh2-hps-phi and pBHR70	This study

2.6. Gene Expression in *E. coli* and Protein Purification

The *E. coli* strain BL21 (DE3) with constructed pET-28a vectors grew in lysogeny broth (400 mL; Sangon Biotech Co., Ltd., Shanghai, China) at 37 °C and 200 rpm with 50 µg/mL kanamycin (Solarbio Science & Technology Co., Ltd., Beijing, China) to an absorbance ranging from 0.6 to 0.8 (600 nm). Gene expression was induced by adding 0.1 mM isopropyl- β -D-thiogalactopyranoside (Solarbio Science & Technology Co., Ltd., Beijing, China), and the cells were incubated at 18 °C for 16 h. The bacterial cells were harvested by centrifugation (10,000 \times g for 30 min at 4 °C) and re-suspended in a lysis buffer (20 mM imidazole, 50 mM Tris HCl, 150 mM NaCl (Solarbio, Beijing, China; pH = 7.5)). The cells were disrupted by passing the cell suspension three times through a high-pressure homogenizer (JN-3000 PLUS) at 6,894,757 Pa (1000 Psi). Cell debris and membrane fractions were removed by centrifugation (10,000 \times g for 30 min at 4 °C). The supernatant was loaded onto a Ni-NTA agarose column (GE Healthcare Bio-Sciences AB, Uppsala, Sweden) equilibrated with the lysis buffer (20 mM imidazole, 50 mM Tris HCl, 150 mM NaCl; pH = 7.5). The column was washed with 2 column volumes of the lysis buffer and 2 column volumes of the wash buffer (50 mM imidazole, 50 mM Tris HCl, 150 mM NaCl; pH = 7.5). The proteins were finally eluted with a gradient elution buffer ((100 mM, 150 mM, 200 mM, respectively) imidazole, 50 mM Tris HCl, 150 mM NaCl; pH = 7.5). The purified proteins were desalted using an ultrafiltration tube (10,000 MWCO; Millipore, Burlington, MA, USA) with a desalting buffer (50 mM Tris HCl, 150 mM NaCl, 6 mM MgCl₂; pH = 7.5) [31]. Protein concentration was determined using the Bradford method [32] with a BCA Protein Assay Kit (Solarbio, Beijing, China), and the sizes of the standard and protein enrichments were confirmed through sodium dodecyl sulfate–polyacrylamide gel electrophoresis (SDS–PAGE).

2.7. Enzyme Activity Measurement

2.7.1. Assay of NAD-Dependent Methanol Dehydrogenase Activity In Vitro

The reaction was conducted in 3-paralleled 200 µL in pre-heated (37 °C) 50 mM K₂HPO₄ buffer containing 5 mM MgSO₄, 500 µM NAD⁺ (all purchased from Sigma-Aldrich, St. Louis, MO, USA), and 200 µg protein; 0.5 M methanol (Sigma-Aldrich, St. Louis, MO, USA) was added [10]. The production of NADH was measured at 340 nm and 37 °C with a microplate reader (Infinite 200 PRO; Tecan, Zurich, Switzerland) every minute until a steady state was reached. Average values were used to calculate the activity of enzymes in vitro according to a standard curve of NADH at different concentrations combining the reading sample time. One unit (U) was defined as the amount of enzyme required to process 1 mM of substrate per minute, and specific units (U/mg protein) were calculated by the total protein concentration [10].

2.7.2. Assay of Hps-phi Fusion Activity In Vitro

The fused enzyme activity of purified Hps-phi was assayed by measuring the NADPH formation via coupled reactions catalyzed by glucose-6-phosphate dehydrogenase (G6PD) and phosphoglucosomerase (Pgi) at 37 °C as described previously [33,34]. Subsequently, 5 mM ribose-5-phosphate (Sigma-Aldrich, St. Louis, MO, USA) was used as the initial substrate to convert the reaction mixture of 200 µL to ribulose-5-phosphate by 10 U Pgi at 37 °C for 5 min to start the reaction. The reaction mixture contained 50 mM K₂HPO₄,

2.5 mM NADP⁺, 5 mM MgSO₄, 10 U G6PD, and 10 U Pgi. To start the reaction, 5 mM formaldehyde was added to the reaction mixture. Each sample was tested in 3 parallels.

2.7.3. Enzyme Activity Measurement by Formaldehyde Production/Consumption In Vivo

Enzyme activity assay for methanol dehydrogenase and Hps-phi was conducted in vivo using a method similar to that described in the study by Muller et al. [10]. Cells were grown overnight in a Murashige and Skoog (MS) medium supplemented with 0.5% ribose (We tested whether ribose could produce more pentose as ribulose could not be purchased. Pentose was preferable for methanol assimilation; data not shown.) and antibiotics. Up to 200 µL supernatant was mixed with Nash's reagent [35], and the formaldehyde concentration was determined at 412 nm with a microplate reader. The activity was calculated similarly to NAD-dependent methanol dehydrogenase activity in vitro. One unit (U) was defined as 1 mmol formaldehyde produced per minute. For calculating specific units (U/mg protein), the protein concentration was estimated based on the OD₆₀₀ of the culture and the assumption that 1 L culture with an OD₆₀₀ of 1 contains 0.250 g of biomass, half of which was assumed to be protein.

2.7.4. PHB Production and Assay of PHB

Constructed *E. coli* strains were grown overnight in an LB medium with antibiotics. The following morning, 1 mL bacteria solution was used to inoculate in main cultures containing 50 mL of MS medium with 100 mM ribose (Sigma-Aldrich, St. Louis, MO, USA) in 250 mL baffled shake flasks to an OD₆₀₀ of 0.8. Subsequently, 0.1 mM IPTG was added to the solution. Cells were grown at 20 °C, shaking at 220 rpm for 10 h.

Cells were centrifuged at 10,000× g for 4 min at room temperature and re-suspended with water. They were then centrifuged and re-suspended twice. The pellet was re-suspended in 50 mL standard MS medium without glucose or ribose, and the actual OD₆₀₀ was measured. The re-suspended cells were inoculated at 37 °C, shaking at 150 rpm as 0.5 M methanol was added. After inoculation for 22 h, the re-suspended cells (pelleted by centrifugation at 10,000× g for 4 min at 4 °C) were freeze-dried to determine the PHB concentration.

The PHB content (*w/w* %) was quantified by gas chromatography (GC5; Persee, Beijing, China) with an HP-5 capillary column [36,37]. The PHB content (*w/w* %) was defined as the percent ratio of PHB concentration (dry weight per liter of culture broth) to cell concentration (dry weight per liter of culture broth).

3. Results

3.1. Prediction of Optimal PHB Production Pathway

The optimal PHB pathway and flux distribution from RuMP and MCC calculated by the extended *E. coli* metabolic model iML1515 is shown in Figure 1. After adding the RuMP pathway (Mdh, Hps-phi) and PHB synthetic pathway (PhaA, PhaB and PhaC) to iML1515, the PHB production rate was calculated as 1 mmol/gDCW/h PHB (C4) from 6 mmol/gDCW/h methanol (C1) (Figure 1A). Methanol was converted to PHB with carbon loss as CO₂ at the pyruvate decarboxylation step, leading to the C-mol yield of PHB of 0.67 using the RuMP pathway. After adding the NOG pathway (FxpK) to form the MCC pathway, the PHB production rate was improved to 1.5 mmol/gDCW/h from 6 mmol/gDCW/h methanol consumption (Figure 1B). This rate was equal to 1 C-mol/C-mol carbon yield, which was a 50% increase relative to a C-mol yield of 0.67 obtained from the RuMP pathway. This result implied that the combination of the NOG pathway with the RuMP pathway could theoretically improve PHB yield from methanol in *E. coli*.

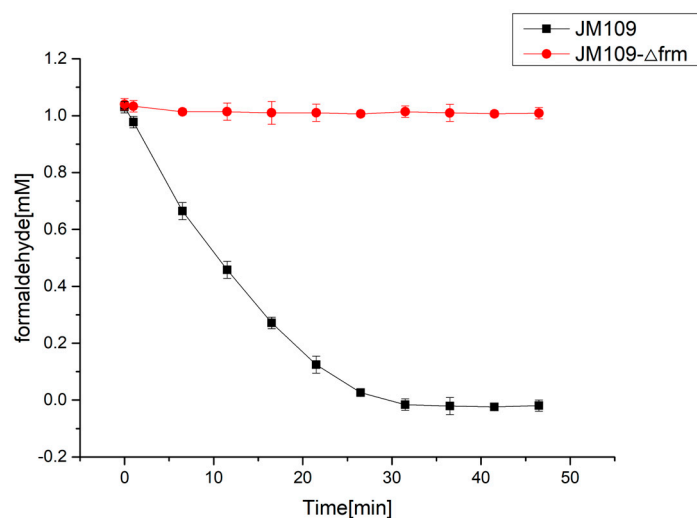


Figure 2. Formaldehyde degradation in *E. coli* JM109 strain (black symbols) and JM109-Δfrm strain (red symbols). The result indicated that the deletion of *frmA* is important to accumulate enough formaldehyde as the substrate for RuMP pathway. All experiments were conducted in triplicate. The mean values of three biological replicates are presented, and error bars indicate standard deviations.

3.3. Construction of C1 Assimilation Module

The C1 assimilation module included methanol dehydrogenase and the fused Hps-phi enzyme. The Hps-phi enzyme was chosen based on the study by Orita et al. [24], which reported a considerably high activity. The Hps-phi activities measured in vitro and in vivo (4400 and 1602 mU/mg, respectively; Table 3) in our study were similar to the previously reported values. By contrast, the reported Mdh enzyme activities were very considerably low [10]. To find an Mdh enzyme with high activity, we tested three Mdh enzymes from *B. methanolicus* MGA3, *T. acidophilum* DSM 1728, and *C. necator* N-1, respectively. The results shown in Table 3 indicate that Mdh from *B. methanolicus* (encoded by the *mdh2* gene) exhibits the highest activity both in vitro (11.4 mU/mg) and in vivo (9.2 mU/mg). Therefore, *mdh2* was selected to construct the C1 assimilation module in the engineered strains.

Table 3. Measured activities of different enzymes from different sources. In vitro activities were measured using purified proteins; in vivo activities were measured using *E. coli* cell suspensions harboring the corresponding enzymes. Description contains the advantages of each enzyme mentioned in the literature. The hyphen (-) indicates activity not detected. Sources column specifies the species source of these enzymes. Shown are the mean values of three biological replicates.

Enzyme Activity (mU/mg)	In Vitro	In Vivo	Description	Sources	Reference
mdh2	11.4	9.2	Higher activity in vivo	<i>B. methanolicus</i> MGA3	[10]
TaADH (Ta1316 ADH)	0.9	-	High relative activity in vitro at high temperature	<i>T. acidophilum</i> DSM 1728	[23]
mdh-CT	4.8	0.43	Higher activity in vitro	<i>C. necator</i> N-1	[22]
Hps-phi	4400	1602	Higher efficiency than a simple mixture of individual enzymes	<i>M. gastri</i> MB19	[24]

To evaluate the effect of the C1 assimilation module, genes encoding the enzymes Mdh and fused Hps-phi were orderly integrated into an expression vector pZQ to generate vectors pZQ_mdh2 and pZQ_mdh2-hps-phi (Table 1). Then these two vectors were transformed into JM109-Δfrm to construct the JM109-Δfrm-mdh2 and JM109-Δfrm-C1, respectively. Then, formaldehyde concentrations for different strains in methanol media were measured (Figure 3). The results indicated that the introduction of *mdh2* could successfully

enable the conversion of methanol to formaldehyde in strain JM109- Δ frm-mdh2, whereas the formaldehyde could not be further utilized. With the further introduction of Hps-phi fusion, the formaldehyde concentration could be reduced in strain JM109- Δ frm-C1, which indicated that formaldehyde was converted into the RuMP pathway. However, a significant amount of formaldehyde remained that could be utilized. This might be owing to the lack of ribulose-5-phosphate, which was a key intermetabolite for the condensation of formaldehyde (Figure 1). As we failed to obtain a relatively inexpensive Ru5P as a carbon source, an alternative method using ribose to supply ribulose-5-phosphate, ribose-5-phosphate, and other circulating C5 metabolites by cellular metabolism was tested. An obvious decrease in formaldehyde concentration was observed in strain JM109- Δ frm-C1 using ribose and methanol as carbon sources. This demonstrated that the expression of enzyme Hps-phi fusion was effective for the conversion of formaldehyde into the central pathways when circulating C5 metabolites were relatively sufficient.

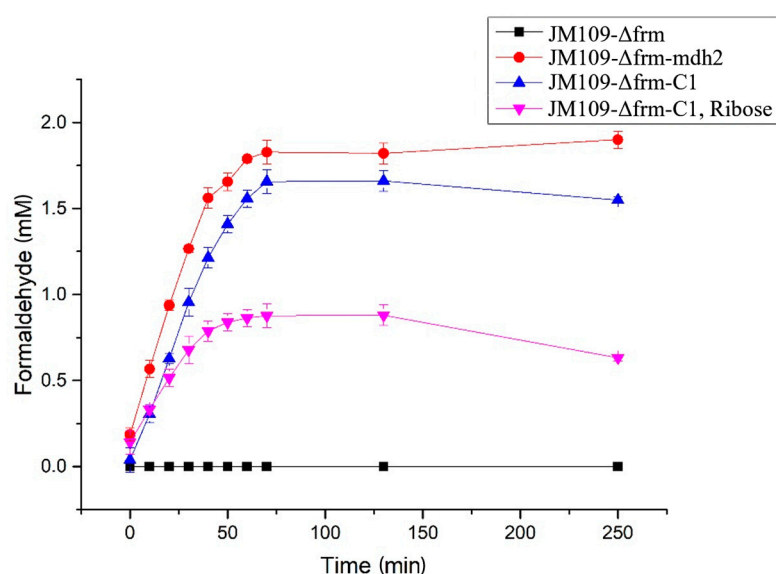


Figure 3. Formaldehyde production in JM109- Δ frm cells expressing *mdh2* in the presence or absence of *hps-phi* fusion. The strain JM109- Δ frm (black squares), which did not contain constructed plasmids, was set as control. The strain JM109- Δ frm-mdh2 (red circles), which contained Mdh2 enzyme, was set to test whether Mdh2 could convert methanol to formaldehyde. The strain JM109- Δ frm-C1 (blue triangles), which contained enzymes Mdh2 and Phs-phi fusion, was set to test whether formaldehyde generated from methanol could be further assimilated into RuMP pathway. Ribose was added as an alternative method to supply circulating C5 metabolites (pink inverted triangles). The mean values of three biological replicates are shown, and error bars indicate standard deviations.

3.4. Evaluation of the Effect of C1 and NOG Module on PHB Production from Methanol

The construction of plasmid pBHR68 for PHB production (including *phaA*, *phaB*, and *phaC*) was conducted in a previous study [26]. We used the plasmid pBHR68 as the PHB production module. This plasmid was transformed into JM109- Δ frm and JM109- Δ frm-C1 to obtain new strains JM109- Δ frm-PHB and JM109- Δ frm-C1-PHB, respectively. The strain JM109- Δ frm-PHB, which contained only the PHB production module but not the C1 module, was also created as a control. JM109- Δ frm-C1-PHB contained all the required genes for converting methanol to PHB. As shown in Figure 1, the C1 assimilation module needed to combine well with the NOG module (phosphoketolase) to form the complete carbon-conserved pathway. We then further introduced the phosphoketolase gene *fxpk* from *Bifidobacterium adolescentis* into the genome of JM109- Δ frm-C1-PHB, obtaining the strain JM109-NOG- Δ frm-C1-PHB. To increase the Fxpk expression, the *fxpk* gene was also inserted into the PHB synthesis plasmid pBHR68 for the formation of a new plasmid, pBHR70.

Plasmid PBHR70, replacing PBHR68, was introduced into JM109-NOG- Δ frm-C1 to obtain a new strain JM109-NOG- Δ frm-C1-PHB-NOG with improved phosphoketolase expression.

To evaluate whether the C1 and NOG modules contribute to PHB biosynthesis, PHB production was conducted with or without methanol (Figure 4). A statistical analysis of the obtained data was performed using SPSS 18.0 for Windows, and differences between the production with or without methanol were evaluated using a *t*-test, where $p < 0.05$ was considered significantly different. When the C1 absorption function module was absent, the addition of methanol would not increase the yield of PHB in strain JM109- Δ frm-PHB. By contrast, the content of PHB in strain JM109- Δ frm-C1-PHB increased by 7.4% (from 3.27% to 3.51%) when supplied with methanol. Moreover, the PHB content of JM109- Δ frm-C1-PHB strain on methanol (3.51%) was higher than that of the control group JM109- Δ frm-PHB (3.39%). These results indicated that methanol was indeed converted to PHB with the addition of the C1 module. However, both the increases in PHB content were relatively low, implying that the classic RuMP pathway, solely, might not be sufficient for efficient PHB biosynthesis from methanol in *E. coli*.

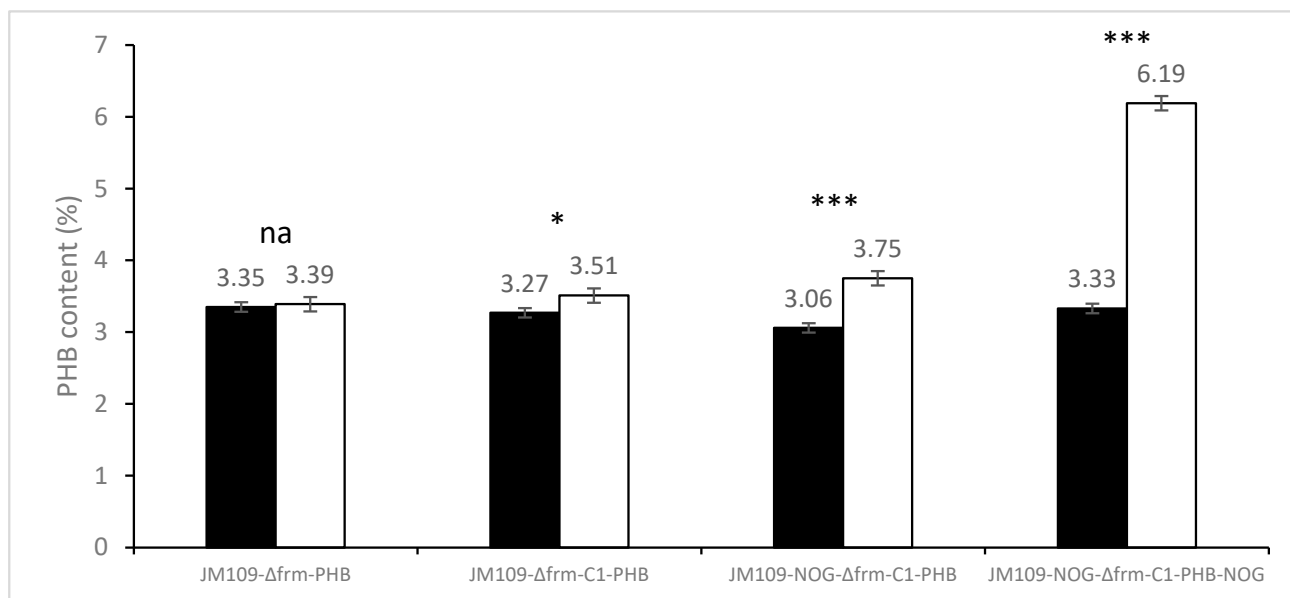


Figure 4. PHB production from different engineered *E. coli* strains. The introduction of the phosphoketolase gene to form the complete MCC pathway greatly improved PHB content. JM109- Δ frm-PHB with only PHB production module was set as control. JM109- Δ frm-C1-PHB with PHB production module and C1 assimilation module was set to test the RuMP pathway. JM109-NOG- Δ frm-C1-PHB with PHB production module, C1 assimilation module, and low-expression NOG module was set to test the MCC pathway. JM109-NOG- Δ frm-C1-PHB-NOG with PHB production module, C1 assimilation module, and high-expression NOG module was also set to test the MCC pathway. Shown are the mean values of three biological replicates, and error bars indicate standard deviations. The dark and white columns represented engineered strains conducted using water and methanol, respectively. *t*-tests were conducted to evaluate statistical significance at $p < 0.05$ (*), and $p < 0.001$ (***).

After the introduction of the NOG module, the PHB content of JM109-NOG- Δ frm-C1-PHB strain in the methanol group (3.75%) was about 22.5% higher than that in the non-methanol group (3.06%). The PHB content of strains with the NOG module (3.75%) was 6.8% higher than that of strains without the NOG module (3.51%) with methanol as a carbon source, which indicated that the addition of the NOG module could facilitate PHB biosynthesis from methanol. With the further overexpression of the NOG module using multi-copy plasmid in strain JM109-NOG- Δ frm-C1-PHB-NOG, its PHB content from methanol (6.19%) was 85% higher than that without methanol (3.33%) and was 65.1% higher than that produced by JM109-NOG- Δ frm-C1-PHB (3.75%). This indicated that

the expression level of NOG is important in the methanol bioconversion using the MCC pathway. The comparison of the above results shows that the overexpression of the MCC pathway can significantly facilitate PHB biosynthesis from methanol, which is consistent with the *in silico* calculation result.

4. Discussion

Considering the low cost of methanol and the continuing efforts to convert abundant natural gas and coal into methanol, developing technologies to convert methanol into other industrial products has drawn interest [12]. In recent decades, several studies have reported on the use of methylotrophs for industrial chemical production from methanol [4–7].

Muller et al. [10] were the first to demonstrate the possibility of using methanol in engineered *E. coli* by introducing the Mdh and RuMP genes into the host. Whitaker et al. [8] further optimized the engineered strain using a superior Mdh from *B. stearothersophilus* and demonstrated that the engineered strain could convert methanol to flavanone naringenin. However, both studies used the natural RuMP pathway for methanol assimilation, which is not favorable for the production of acetyl-CoA-derived products (such as PHB) resulting from carbon loss during pyruvate decarboxylation, as described by Bogorad et al. [11].

On the basis of previous studies and guided by the optimal pathway for PHB production determined by genome-scale network analysis, we first engineered the MCC pathway in *E. coli* to improve product yield. The MCC pathway is the combination of the RuMP pathway with the NOG pathway [40], which can theoretically enable 100% carbon conservation from methanol to acetyl-CoA-derived products.

To evaluate whether the MCC pathway is better than the RuMP pathway in C1 utilization, we first selected the candidate enzymes by testing the activities of the enzymes (Table 3) *in vivo* and *in vitro*. As a result, *mdh2* from *B. methanolicus* MGA3 and Hps-phi fusion [24] were selected as C1 assimilation enzymes in this study. Compared with previously reported results [9,24], the results on the enzyme activities in the present study are similar; the candidate enzymes we selected would be effective for the host. The *frmA* gene coded the enzyme converting formaldehyde to formate would greatly reduce the availability of formaldehyde to Hps-phi (Figure 3) if the gene existed. Three types of modules, C1 assimilation modules, NOG modules, and PHB production modules (Figure 1), were then constructed. The three modules could build the MCC pathway in the host with corresponding enzymes (Table 1), and the effect of the C1 assimilation module was confirmed (Figure 4).

The construction of the MCC pathway has also been conducted *in vitro* [11], which could continuously produce ethanol. However, it could not achieve the complete conversion to products because of the accumulation of intermediary metabolites. In the present study, the formaldehyde generated from methanol could not be completely consumed further (Figure 3). This might be due to the insufficient supply of circulating metabolites, such as ribulose-5-phosphate and xylulose-5-phosphate, which have been reported to be an important factor in methanol bioconversion via the RuMP pathway [9]. Since the construction of *E. coli* strains that can grow with methanol as the sole carbon source is still difficult [9], in this study, the PHB biosynthesis from methanol was conducted via whole-cell biocatalysis (Figure 4). Although the final PHB content from methanol (6.19%) was not as high as those previously reported (ranging from 20% to 29% PHB content) from sugar-based carbon sources [26] or other carbon sources [41–43], a significant increase of 65% in PHB content with the MCC pathway was observed relative to that with only the RuMP pathway through statistical analysis. The experimental results confirm the importance of the combination of NOG with RuMP to form the complete MCC pathway, which can obviously facilitate the biosynthesis of acetyl-CoA-derived chemicals from one-carbon compounds. Future efforts can be expected to engineer cellular metabolism for growable strains via the MCC pathway using a one-carbon compound as the sole carbon source.

5. Conclusions

On the basis of metabolic network analysis, we found that the MCC pathway can convert C1 compounds into acetyl-CoA-derived products, such as PHB, without carbon loss. We engineered this pathway in *E. coli* by introducing the heterologous genes for C1 assimilation, phosphoketolase (NOG), and PHB production from different organisms. Compared with the strain containing only the RuMP pathway for C1 assimilation, the strain with the complete MCC pathway produced more PHB by assimilating methanol. Despite the low PHB content relative to that from strains growing on glucose, the results indicate that the introduction of the MCC pathway in *E. coli* can improve its ability for C1 compound bioconversion. To our knowledge, the present study is the first metabolic engineering research on the conversion of methanol to PHB in *E. coli*. This study provides a basis for subsequent studies to further improve product yield from methanol.

Supplementary Materials: The following supporting information can be downloaded at: <https://www.mdpi.com/article/10.3390/bioengineering10040415/s1>, Table S1: Primer sequences used in this study.

Author Contributions: Conceptualization, Z.C. and H.M.; methodology, Z.C. and J.W.; formal analysis, X.D. and J.W.; investigation, Z.C. and Q.Y.; resources, H.M.; writing—original draft preparation, Z.C.; writing—review and editing, J.W., X.D., Q.Y. and H.M.; visualization, X.D.; supervision, Q.Y. and H.M.; project administration, H.M. All authors have read and agreed to the published version of the manuscript.

Funding: This research was funded by the National Key Research and Development Program of China (2018YFA09013400), the National Natural Science Foundation of China (21908239), and the Tianjin Synthetic Biotechnology Innovation Capacity Improvement Project (TSBICIP-PTJS-001).

Institutional Review Board Statement: Not applicable.

Informed Consent Statement: Informed consent was obtained from all subjects involved in the study.

Data Availability Statement: Not applicable.

Conflicts of Interest: The authors declare no conflict of interest.

References

1. Patel, S.K.S.; Gupta, R.K.; Kalia, V.C.; Lee, J.-K. Integrating anaerobic digestion of potato peels to methanol production by methanotrophs immobilized on banana leaves. *Bioresour. Technol.* **2021**, *323*, 124550. [CrossRef] [PubMed]
2. Kumar, V.; Patel, S.K.S.; Gupta, R.K.; Otari, S.V.; Gao, H.; Lee, J.-K.; Zhang, L. Enhanced Saccharification and Fermentation of Rice Straw by Reducing the Concentration of Phenolic Compounds Using an Immobilized Enzyme Cocktail. *Biotechnol. J.* **2019**, *14*, 1800468. [CrossRef] [PubMed]
3. Zezzi do Valle Gomes, M.; Palmqvist, A.E.C. Influence of operating conditions and immobilization on activity of alcohol dehydrogenase for the conversion of formaldehyde to methanol. *New J. Chem.* **2017**, *41*, 11391–11397. [CrossRef]
4. Westlake, R. Large-scale Continuous Production of Single Cell Protein. *Chem. Ing. Tech.* **1986**, *58*, 934–937. [CrossRef]
5. Windass, J.D.; Worsey, M.J.; Pioli, E.M.; Pioli, D.; Barth, P.T.; Atherton, K.T.; Dart, E.C.; Byrom, D.; Powell, K.; Senior, P.J. Improved conversion of methanol to single-cell protein by *Methylophilus methylotrophus*. *Nature* **1980**, *287*, 396–401. [CrossRef] [PubMed]
6. Schrader, J.; Schilling, M.; Holtmann, D.; Sell, D.; Filho, M.V.; Marx, A.; Vorholt, J.A. Methanol-based industrial biotechnology: Current status and future perspectives of methylotrophic bacteria. *Trends Biotechnol.* **2009**, *27*, 107–115. [CrossRef]
7. Brautaset, T.; Jakobsen, O.M.; Josefsen, K.D.; Flickinger, M.C.; Ellingsen, T.E. *Bacillus methanolicus*: A candidate for industrial production of amino acids from methanol at 50 degrees C. *Appl. Microbiol. Biotechnol.* **2007**, *74*, 22–34. [CrossRef]
8. Whitaker, W.B.; Jones, J.A.; Bennett, R.K.; Gonzalez, J.E.; Vernacchio, V.R.; Collins, S.M.; Palmer, M.A.; Schmidt, S.; Antoniewicz, M.R.; Koffas, M.A.; et al. Engineering the biological conversion of methanol to specialty chemicals in *Escherichia coli*. *Metab. Eng.* **2017**, *39*, 49–59. [CrossRef]
9. Sanford, P.A.; Woolston, B.M. Synthetic or natural? Metabolic engineering for assimilation and valorization of methanol. *Curr. Opin. Biotechnol.* **2022**, *74*, 171–179. [CrossRef]
10. Muller, J.E.N.; Meyer, F.; Litsanov, B.; Kiefer, P.; Potthoff, E.; Heux, S.; Quax, W.J.; Wendisch, V.F.; Brautaset, T.; Portais, J.C.; et al. Engineering *Escherichia coli* for methanol conversion. *Metab. Eng.* **2015**, *28*, 190–201. [CrossRef]
11. Bogorad, I.W.; Chen, C.T.; Theisen, M.K.; Wu, T.Y.; Schlenz, A.R.; Lam, A.T.; Liao, J.C. Building carbon-carbon bonds using a biocatalytic methanol condensation cycle. *Proc. Natl. Acad. Sci. USA* **2014**, *111*, 15928–15933. [CrossRef] [PubMed]

12. Haynes, C.A.; Gonzalez, R. Rethinking biological activation of methane and conversion to liquid fuels. *Nat. Chem. Biol.* **2014**, *10*, 331–339. [[CrossRef](#)]
13. Anderson, A.J.; Dawes, E.A. Occurrence, metabolism, metabolic role, and industrial uses of bacterial polyhydroxyalkanoates. *Microbiol. Rev.* **1990**, *54*, 450–472. [[CrossRef](#)]
14. Lee, S.Y. Bacterial polyhydroxyalkanoates. *Biotechnol. Bioeng.* **1996**, *49*, 1–14. [[CrossRef](#)]
15. Williams, S.F.; Martin, D.P.; Horowitz, D.M.; Peoples, O.P. PHA applications: Addressing the price performance issue: I. Tissue engineering. *Int. J. Biol. Macromol.* **1999**, *25*, 111–121. [[CrossRef](#)] [[PubMed](#)]
16. van der Walle, G.A.M.; Buisman, G.J.H.; Weusthuis, R.A.; Eggink, G. Development of environmentally friendly coatings and paints using medium-chain-length poly(3-hydroxyalkanoates) as the polymer binder. *Int. J. Biol. Macromol.* **1999**, *25*, 123–128. [[CrossRef](#)] [[PubMed](#)]
17. Sudesh, K.; Abe, H.; Doi, Y. Synthesis, structure and properties of polyhydroxyalkanoates: Biological polyesters. *Prog. Polym. Sci.* **2000**, *25*, 1503–1555. [[CrossRef](#)]
18. Müller-Santos, M.; Koskimäki, J.J.; Alves, L.P.S.; de Souza, E.M.; Jendrossek, D.; Pirttilä, A.M. The protective role of PHB and its degradation products against stress situations in bacteria. *FEMS Microbiol. Rev.* **2020**, *45*, fuaa058. [[CrossRef](#)]
19. Orth, J.D.; Thiele, I.; Palsson, B.O. What is flux balance analysis? *Nat. Biotechnol.* **2010**, *28*, 245–248. [[CrossRef](#)]
20. Monk, J.M.; Lloyd, C.J.; Brunk, E.; Mih, N.; Sastry, A.; King, Z.; Takeuchi, R.; Nomura, W.; Zhang, Z.; Mori, H.; et al. iML1515, a knowledgebase that computes *Escherichia coli* traits. *Nat. Biotechnol.* **2017**, *35*, 904–908. [[CrossRef](#)]
21. Ebrahim, A.; Lerman, J.A.; Palsson, B.O.; Hyduke, D.R. COBRAPy: COntstraints-Based Reconstruction and Analysis for Python. *BMC Syst. Biol.* **2013**, *7*, 74. [[CrossRef](#)] [[PubMed](#)]
22. Wu, T.Y.; Chen, C.T.; Liu, J.T.; Bogorad, I.W.; Damoiseaux, R.; Liao, J.C. Characterization and evolution of an activator-independent methanol dehydrogenase from *Cupriavidus necator* N-1. *Appl. Microbiol. Biotechnol.* **2016**, *100*, 4969–4983. [[CrossRef](#)]
23. Marino-Marmolejo, E.N.; De Leon-Rodriguez, A.; de la Rosa, A.P.; Santos, L. Heterologous expression and characterization of an alcohol dehydrogenase from the archeon *Thermoplasma acidophilum*. *Mol. Biotechnol.* **2009**, *42*, 61–67. [[CrossRef](#)] [[PubMed](#)]
24. Orita, I.; Sakamoto, N.; Kato, N.; Yurimoto, H.; Sakai, Y. Bifunctional enzyme fusion of 3-hexulose-6-phosphate synthase and 6-phospho-3-hexuloisomerase. *Appl. Microbiol. Biotechnol.* **2007**, *76*, 439–445. [[CrossRef](#)]
25. Engler, C.; Kandzia, R.; Marillonnet, S. A one pot, one step, precision cloning method with high throughput capability. *PLoS ONE* **2008**, *3*, e3647. [[CrossRef](#)] [[PubMed](#)]
26. Spiekermann, P.; Rehm, B.H.; Kalscheuer, R.; Baumeister, D.; Steinbuchel, A. A sensitive, viable-colony staining method using Nile red for direct screening of bacteria that accumulate polyhydroxyalkanoic acids and other lipid storage compounds. *Arch. Microbiol.* **1999**, *171*, 73–80. [[CrossRef](#)] [[PubMed](#)]
27. Silva-Rocha, R.; Martínez-García, E.; Calles, B.; Chavarría, M.; Arce-Rodríguez, A.; de Las Heras, A.; Páez-Espino, A.D.; Durante-Rodríguez, G.; Kim, J.; Nikel, P.I.; et al. The Standard European Vector Architecture (SEVA): A coherent platform for the analysis and deployment of complex prokaryotic phenotypes. *Nucleic Acids Res.* **2013**, *41*, D666–D675. [[CrossRef](#)]
28. Kuhlman, T.E.; Cox, E.C. Site-specific chromosomal integration of large synthetic constructs. *Nucleic Acids Res.* **2010**, *38*, e92. [[CrossRef](#)]
29. Yang, X.; Yuan, Q.; Zheng, Y.; Ma, H.; Chen, T.; Zhao, X. An engineered non-oxidative glycolysis pathway for acetone production in *Escherichia coli*. *Biotechnol. Lett.* **2016**, *38*, 1359–1365. [[CrossRef](#)]
30. Datsenko, K.A.; Wanner, B.L. One-step inactivation of chromosomal genes in *Escherichia coli* K-12 using PCR products. *Proc. Natl. Acad. Sci. USA* **2000**, *97*, 6640–6645. [[CrossRef](#)]
31. Wen, L.; Huang, K.; Liu, Y.; Wang, P.G. Facile Enzymatic Synthesis of Phosphorylated Ketopentoses. *ACS Catal.* **2016**, *6*, 1649–1654. [[CrossRef](#)]
32. Kruger, N.J. The Bradford method for protein quantitation. *Methods Mol. Biol.* **1994**, *32*, 9–15. [[PubMed](#)]
33. Yasueda, H.; Kawahara, Y.; Sugimoto, S. *Bacillus subtilis* yckG and yckF encode two key enzymes of the ribulose monophosphate pathway used by methylotrophs, and yckH is required for their expression. *J. Bacteriol.* **1999**, *181*, 7154–7160. [[CrossRef](#)] [[PubMed](#)]
34. Lessmeier, L.; Pfeifenschneider, J.; Carnicer, M.; Heux, S.; Portais, J.C.; Wendisch, V.F. Production of carbon-13-labeled cadaverine by engineered *Corynebacterium glutamicum* using carbon-13-labeled methanol as co-substrate. *Appl. Microbiol. Biotechnol.* **2015**, *99*, 10163–10176. [[CrossRef](#)]
35. Nash, T. The colorimetric estimation of formaldehyde by means of the Hantzsch reaction. *Biochem. J.* **1953**, *55*, 416–421. [[CrossRef](#)]
36. Abe, H.; Doi, Y.; Fukushima, T.; Eya, H. Biosynthesis from gluconate of a random copolyester consisting of 3-hydroxybutyrate and medium-chain-length 3-hydroxyalkanoates by *Pseudomonas* sp. 61-3. *Int. J. Biol. Macromol.* **1994**, *16*, 115–119. [[CrossRef](#)] [[PubMed](#)]
37. Liu, Q.; Lin, Z.; Zhang, Y.; Li, Y.; Wang, Z.; Chen, T. Improved poly(3-hydroxybutyrate) production in *Escherichia coli* by inactivation of cytochrome bd-II oxidase or/and NDH-II dehydrogenase in low efficient respiratory chains. *J. Biotechnol.* **2014**, *192 Pt A*, 170–176. [[CrossRef](#)]
38. Gutheil, W.G.; Holmquist, B.; Vallee, B.L. Purification, characterization, and partial sequence of the glutathione-dependent formaldehyde dehydrogenase from *Escherichia coli*: A class III alcohol dehydrogenase. *Biochemistry* **1992**, *31*, 475–481. [[CrossRef](#)]
39. Gonzalez, C.F.; Proudfoot, M.; Brown, G.; Korniyenko, Y.; Mori, H.; Savchenko, A.V.; Yakunin, A.F. Molecular basis of formaldehyde detoxification. Characterization of two S-formylglutathione hydrolases from *Escherichia coli*, FrmB and YeiG. *J. Biol. Chem.* **2006**, *281*, 14514–14522. [[CrossRef](#)]

40. Bogorad, I.W.; Lin, T.S.; Liao, J.C. Synthetic non-oxidative glycolysis enables complete carbon conservation. *Nature* **2013**, *502*, 693–697. [[CrossRef](#)]
41. Li, H.F.; Tian, L.; Lian, G.; Fan, L.H.; Li, Z.J. Engineering *Vibrio alginolyticus* as a novel chassis for PHB production from starch. *Front. Bioeng. Biotechnol.* **2023**, *11*, 1130368. [[CrossRef](#)] [[PubMed](#)]
42. Yim, S.S.; Choi, J.W.; Lee, Y.J.; Jeong, K.J. Rapid combinatorial rewiring of metabolic networks for enhanced poly(3-hydroxybutyrate) production in *Corynebacterium glutamicum*. *Microb. Cell Fact.* **2023**, *22*, 29. [[CrossRef](#)] [[PubMed](#)]
43. Saeed, S.; Firyal, S.; Tayyab, M.; Irfan, M.; Mohy ud Din, A.; Mehmood, T. Bioconversion of apple peels (*Malus domestica*) to polyhydroxybutyrate using statistical design to optimize process parameters through *Bacillus thuringiensis* via solid-state fermentation. *Biomass Convers. Biorefinery* **2022**. [[CrossRef](#)]

Disclaimer/Publisher's Note: The statements, opinions and data contained in all publications are solely those of the individual author(s) and contributor(s) and not of MDPI and/or the editor(s). MDPI and/or the editor(s) disclaim responsibility for any injury to people or property resulting from any ideas, methods, instructions or products referred to in the content.